Food Chemistry 122 (2010) 31–41

Contents lists available at ScienceDirect

Food Chemistry

journal homepage: www.elsevier.com/locate/foodchem

Sesquiterpenoids with free-radical-scavenging properties from marine macroalga *Ulva fasciata* Delile

Kajal Chakraborty *, R. Paulraj

Marine Biotechnology Division, Central Marine Fisheries Research Institute, Ernakulam North, P.O., P.B. No. 1603, Cochin, Kerala 682018, India

ARTICLE INFO

Article history:
Received 30 May 2009
Received in revised form 2 December 2009
Accepted 3 February 2010

Keywords:
Ulva fasciata Delile
Ulvaceae
Sesquiterpenoides
Antioxidant activity

ABSTRACT

Free-radical-scavenging activities of various solvent extracts of *Ulva fasciata*, a chlorophytan marine macroalga with significance as a food ingredient, from the southwestern coast of the Indian peninsula, were evaluated using *in vitro* tests, including 1,1-diphenyl-2-picrylhydrazyl (DPPH) and 2,2′-azino-bis(3-ethylbenzothiazoline-6-sulfonate) (ABTS) scavenging assays. Ethyl acetate (EtOAc) extract of *Ulva fasciata* displayed markedly stronger DPPH (89.8 ± 4.2%) and $ABTS^{\cdot+}$ scavenging (82.6 ± 3.7%) activities at 0.1 mg/ml than dichloromethane and *n*-hexane extracts. Radical scavenging assay-guided chromatographic separation of the EtOAc extract, using a step gradient of petroleum ether/EtOAc yielded five major sesquiterpenoids. After 8 min of incubation the $ABTS^{\cdot+}$ scavenging activity of one of these sesquiterpenoids was higher (71.4 ± 1.5%) than that of Trolox (44.1 ± 1.5%), and therefore may have potential as a natural antioxidant in the food industry.

1. Introduction

Ulva fasciata Delile is a chlorophytan marine macroalga, which grows abundantly in the coastal waters of South India. Marine macroalgae have been identified in both inter-tidal and deep water regions, and proven to be rich sources of structurally diverse bioactive compounds with valuable biomedical potential (Satoru, Noboru, Hiroo, Shinji, & Hiroshi, 2003). Marine green algae *viz.*, *Ulva* sp., are an important food source in many south-east Asian countries (Rouxel et al., 2001). *Ulva fasciata* and *Ulva lactuca* are used in soups and salads, and have been reported to possess antioxidant and antibacterial properties (Beach, Smith, Michael, & Shin, 1995; Rouxel et al., 2001). *Ulva* spp. are very high in Fe, protein, essential amino acids, I_2, Mn, Se, Ni, and vitamins; they exhibit anti-peroxidative and anti-hyperlipidaemic properties (Sathivel, Raghavendran, Srinivasan, & Devaki, 2008).

Recently, much research attention has been focused on the free-radical-scavenging activity of metabolites from marine macroalgae. It is well known that reactive oxygen species are a predominant cause of qualitative decay of food and feed leading to rancidity, toxicity, and destruction of lipid biomolecules important in metabolism (Kim et al., 1998). However the absence of photodynamic damage in the structural components of macroalgae despite being exposed to intense light and high oxygen concentrations implies that their cells possess antioxidative defence mechanisms (Dykens, Shick, Benoit, Buettner, & Winston, 1992; Matsukawa et al., 1997; Ramarathnam, Osawa, Ochi, & Kawakishi, 1995). Among macroalgal natural antioxidants, terpenoids, phlorotannins, polyphenols, phenolic acids, anthocyanins, hydroxycinnamic acid derivatives, and flavonoids are important (Bandoniene & Murkovic, 2002). Antioxidant effect was observed with a sulfoglycolipid fraction isolated from *Porphyridum creuntum* (Berge, Debiton, Dumay, Durand, & Barthomeuf, 2002). Extracts from several macroalgae harvested in Spain (Jiménez-Escrig, Jiménez-Jiménez, Pulido, & Saura-Calixto, 2001), Korea (Han, Lee, & Sung, 1999), China (Yan, Nagata, & Fan, 1998) and Japan (Yan, Chuda, Suzuki, & Nagata, 1999) have demonstrated antioxidant activity *in vitro*. The extracts of macroalga *Taonia atomaria* exhibited high radical-scavenging activity due to the compounds stypodiol and stypoldione (Mayer & Lehmann, 2000). Sargaquinoic acid from brown macroalga *Sargassum macrocarpum* has been found to possess antioxidant activity (Tsang & Kamei, 2004), and therefore may be a potential food supplement.

Currently, reactive oxygen species and lipid oxidation in food industry are being controlled or minimised by the addition of synthetic antioxidants (Gray, Gomaa, & Buckley, 1996). However, with safety concerns about synthetic antioxidants (Wichi et al., 1998), considerable interest has arisen in finding alternative sources of antioxidants for use in food systems. In this paper, we report the solvent extraction, radical scavenging assay-guided chromatographic purification, and structural elucidation of five sesquiterpenoids from *Ulva fasciata* Delile, and elucidate the antioxidant potential of the purified compounds by *in vitro* reactive oxygen species scavenging assays.

* Corresponding author. Tel.: +91 484 2394867; fax: +91 484 2394909.
E-mail address: kajal_iari@yahoo.com (K. Chakraborty).

0308-8146/$ - see front matter © 2010 Elsevier Ltd. All rights reserved.
doi:10.1016/j.foodchem.2010.02.012

2. Materials and methods

2.1. Chemicals and instrumentation

Fourier-transform infrared (FTIR) spectra of KBr pellets were recorded using a Perkin–Elmer Series 2000 FTIR spectrophotometer scanning between 4000 and 400 cm^{-1}. ^1H and ^{13}C NMR spectra were recorded on a Bruker Avance DPX 300 (300 MHz) spectrometer in $CDCl_3$ or DMSO-d_6 as aprotic solvent at ambient temperature with TMS as the internal standard. Standard pulse sequences were used for DEPT, ^1H–^1H–COSY, two-dimensional NOESY, HMQC, and HMBC experiments. The GC analyses were accomplished on a Perkin-Elmer gas chromatograph equipped with an Elite 5 capillary column (30 m × 0.53 mm i.d.) using a flame ionisation detector (FID) equipped with a split/splitless injector, which was used in the split (1:15) mode. The oven temperature ramp program was: 60 °C for 10 min, rising at 5 °C/min to 220 °C; injector and detector temperatures 250 °C; carrier gas N_2 (ultra high purity >99.99%, 3 ml/min). The injection volume was 1 μl. The GC–MS analyses were performed in electronic impact ionisation mode using a Varian GC (CP-3800) interfaced with a Varian 1200L single quadrupole mass spectrometer. The GC was equipped with a DB-5 column (30 m × 0.25 mm i.d.; Agilent, Santa Clara, CA). The carrier gas was ultra high purity He. The injector and detector temperatures were maintained at 300 °C. Samples (1 μl) were injected in split (1:15) mode, and the oven programme was identical to that of the GC-FID analysis. Ion source and transfer line were kept at 300 °C. All compounds were of analytical, spectroscopic or chromatographic reagent grade and were obtained from Merck (Darmstadt, Germany). All reagents and chemical solvents used for products isolation were of analytical grade or higher.

2.2. Algal material and preparation of crude extracts

The samples of *Ulva fasciata* Delile were harvested in winter from an exposed inter-tidal rocky shore in Vizhinjam (south-western India), where it formed dense patches. The fresh samples were washed with sea water followed by fresh water to remove salts, epiphytes, microorganisms and other suspended materials, and stored at −20 °C. Partially air-dried thalli of *U. fasciata* (1600 g) were coarsely powdered, and extracted with methanol (5 l, 95%, v/v) under shaking on a rotary shaker table at 50 °C for 1 week. The methanolic extract was filtered and concentrated *in vacuo* (40–50 °C), to furnish a dark green coloured residue (100 ml), which was fractionated with ethyl acetate (EtOAc). The EtOAc extract after solvent evaporation afforded a brown viscous oily residue (12.6 g, yield 0.79%, with respect to fresh seaweed weight).

2.3. Chromatographic purification of sesquiterpenoids from U. fasciata

An aliquot of the EtOAc extract (4.0 g) was slurried in silica gel (8 g, 60–120 mesh), and loaded into a glass column (90 cm × 4 cm) packed with silica gel (230–400 mesh, 40 g) as adsorbent. The column was initially eluted with petroleum ether (60–80 °C), to remove the waxy material. The eluent polarity was gradually increased by addition of EtOAc (petroleum ether/EtOAc: 19:1, 9:1, 13:3, 4:1, 7:3, 3:2, and 1:1, v/v) to furnish 600 fractions of 30 ml each, which were reduced to 12 groups (F_1–F_{12}) after TLC analysis (petroleum ether:EtOAc, 17:3, v/v). Fraction 3 (F_3) obtained by eluting with petroleum ether:EtOAc (13:3, v/v) was found to be a mixture, which was flash chromatographed on a silica gel column (Biotage, 230–400 mesh, 12 g; Biotage AB, Uppsala, Sweden) using a step gradient of $CHCl_3$:MeOH to afford 250 fractions. Based on analytical TLC, the fractions with similar patterns were pooled together. Compound 5 (22.3 mg, yield 0.56%, with respect to crude EtOAc extract) was eluted with $CHCl_3$:MeOH (95:5, v/v), whereas **2** (18.6 mg, yield 0.47%) was collected as pure compound after eluting with $CHCl_3$:MeOH (97:3, v/v). Fraction 4 (F_4) on chromatography over silica gel (230–400 mesh, 20 g) using Me_2O:$CHCl_3$ (4:1, v/v) afforded **3** (8.9 mg, yield 0.22%). Fraction F_5 was eluted with petroleum ether:EtOAc (7:3, v/v) and rechromatographed using the isocratic solvent system $CHCl_3$:EtOAc (4:1, v/v) on an argentated neutral alumina column ($AgNO_3$ 0.06–0.2 mm, 50 g; EtOH 95% v/v, 150 ml) to afford a mixture containing two components. Preparatory TLC of the mixture on silica gel GF_{254} using *n*-hexane:EtOAc (4:1, v/v) afforded **1** (15.4 mg, yield 0.39%) as major component. Fraction F_1, eluted with petroleum ether:EtOAc (19:1, v/v), was rechromatographed using an argentated neutral alumina column (1.5 × 30 cm), using the isocratic solvent system *n*-hexane:$CHCl_3$ (95:1, v/v) to afford **4** (12.5 mg, yield 0.31%).

2.4. Physicochemical data of the purified compounds

2.4.1. 2,5,5-Trimethyl-4-(4′-methyl-3′-pentenyl)-2-cyclohexen-1-ol (**1**)

Yellowish oil; yield (% dw basis of alga) 1.4 × 10^{-3}; TLC R_f: 0.42 (*n*-hexane:EtOAc 4:1, v/v); GC retention time: 10.25 min.; elemental analysis found: C, 81.12; H, 11.83; O, 7.21 ($C_{15}H_{26}O$ requires C, 81.02; H, 11.79; O, 7.20); UV (CH_3OH), λ_{max} 228 nm; IR ν_{max} (KBr): 3040 (–OH str.), 2962 (methyl–CH str.), 1461, 1035, 820 cm^{-1} (olefinic moiety); ^1H ($CDCl_3$, 300 MHz, δ ppm) and ^{13}C NMR ($CDCl_3$, δ ppm) data, see Table 1A; EIMS *m*/*z* (rel. int.%) 222 [M^+] (7), 206 (10), 194 (15), 191 (42), 178 (52), 138 (71), 126 (82), 112 (100), 70 (72), 52 (23), 24 (12); HRMS (ESI): calcd. for $C_{15}H_{26}O$ 222.3653, found 222.3672.

2.4.2. 4-Isopentyl-3,4,5,5-tetramethyl-2-cyclohexen-1-ol (**2**)

Yellow oil; yield (% dw basis of alga) 1.7 × 10^{-3}; TLC R_f: 0.53 (*n*-hexane:EtOAc 4:1, v/v); GC retention time: 8.20 min.; elemental analysis found: C, 80.35; H, 12.69; O, 7.15 ($C_{15}H_{28}O$ requires C, 80.29; H, 12.58; O, 7.13); UV (CH_3OH), λ_{max} 230 nm; IR ν_{max} (KBr, cm^{-1}): 3360 (–OH), 1259 (C–O), 2775 (methyl CH str.); ^1H ($CDCl_3$, 300 MHz, δ ppm) and ^{13}C NMR ($CDCl_3$, δ ppm) data, see Table 1A; EIMS *m*/*z* (rel. int.%) 224 [M^+] (18), 208 (21), 180 (32), 150 (86), 112 (100), 138 (63), 72 (69), 56 (92); HRMS (ESI): calcd. for $C_{15}H_{28}O$ 224.3811, found 224.3845.

2.4.3. 4-Isopentyl-3,4,5,5-tetramethyl-2-cyclohexen-1-ol (**3**)

Colourless oil; yield (% dw basis of alga) 0.8 × 10^{-3}; TLC R_f: 0.40 (*n*-hexane:EtOAc 4:1, v/v); GC retention time: 12.15 min.; elemental analysis found: C, 80.33; H, 12.67; O, 7.15 ($C_{15}H_{28}O$ requires C, 80.29; H, 12.58; O, 7.13); UV (CH_3OH), λ_{max} 228 nm; IR ν_{max} (KBr): 3500 (–OH), 1270 (C–O cyclohexanone); ^1H ($CDCl_3$, 300 MHz, δ ppm) and ^{13}C NMR ($CDCl_3$, δ ppm) data, see Table 1A; EIMS *m*/*z* (rel. int.%) 224 [M^+] (15), 209 (20), 181 (26), 151 (66), 138 (28), 112 (100), 72 (88), 56 (49), 50 (12), 24 (8); HRMS (ESI): calcd. for $C_{15}H_{28}O$ 224.3811, found 224.3836.

2.4.4. 6-Isopentyl-1,5,5,6-tetramethyl-1-cyclohexene (**4**)

Pale yellow oil; yield (% dw basis of alga) 1.1 × 10^{-3}; TLC R_f: 0.63 (*n*-hexane:EtOAc 4:1, v/v); GC retention time: 7.25 min.; elemental analysis found: C, 86.53; H, 13.69 ($C_{15}H_{28}$ requires C, 86.46; H, 13.54); UV (CH_3OH), λ_{max} 219 nm; IR ν_{max} (KBr): 3341, 1720, 1710, 1452, 1369, 993, 885 cm^{-1}; ^1H ($CDCl_3$, 300 MHz, δ ppm) and ^{13}C NMR ($CDCl_3$, δ ppm) data, see Table 1B; EIMS *m*/*z* (rel. int.%) 208 [M^+] (21), 210 (18), 182 (14), 150 (62), 139 (81), 112 (100), 73 (53), 56 (79); HRMS (ESI): calcd. for $C_{15}H_{28}$ 206.3659, found 206.3682.

Table 1A
NMR spectroscopic data of **1–3** in $CDCl_3$.[a].

C. No.	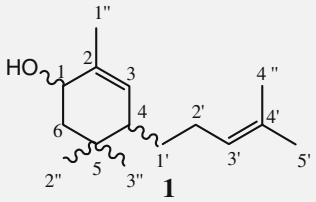 **1**			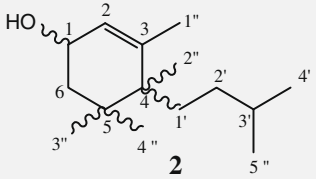 **2**			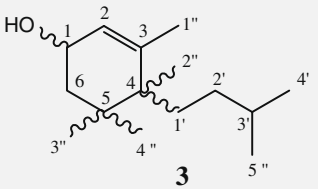 **3**		
	δ^{13}C NMR (DEPT)	H	δ ^{1}H NMR (int., mult., *J* in Hz)[b]	δ^{13}C NMR (DEPT)	H	δ ^{1}H NMR (int., mult., *J* in Hz)[b]	δ^{13}C NMR (DEPT)	H	δ ^{1}H NMR (int., mult., *J* in Hz) [b]
C-1	70.2 (CH)	1α-OH	2.30 (*bs*)	68.4 (CH)	1α-OH	4.21 (*bs*)	64.1 (CH)	1α	3.92 (*dd*, *J* = 7.0 Hz)
	–	1β	3.89 (*t*, *J* = 6.8 Hz)	–	1β	3.89 (*dd*, *J* = 7.5 Hz)	–	1β-OH	4.08 (*bs*)
C-2	132.4 (C)	–	–	123.8 (CH)	2H	5.31 (*d*, *J* = 6.0 Hz)	123.6 (CH)	2H	4.92 (*d*, *J* = 6.0 Hz)
C-3	126.1 (CH)	3H	5.33 (*d*, *J* = 5.9 Hz)	140.2 (C)	–	–	140.7 (C)	–	–
C-4	43.5 (CH)	4β	1.82 (*t*, *J* = 5.8, 6.8 Hz)	52.9 (C)	–	–	51.3 (C)	–	–
C-5	30.9 (C)	–	–	57.1 (C)	–	–	56.5 (C)	–	–
C-6	44.8 (CH_2)	6α	1.53 (*m*)	44.3 (CH_2)	6α	1.52 (*d*, *J* = 5.0 Hz)	43.7 (CH_2)	6α	1.50 (*d*, *J* = 5.0 Hz)
–	–	6β	1.76 (*d*, *J* = 6.8 Hz)	–	6β	1.73 (*t*, *J* = 7.5 Hz)	–	6β	1.52 (*d*, *J* = 7.5 Hz)
C-1′	29.3 (CH_2)	1′α	1.21 (*t*, *J* = 6.0 Hz)	28.2 (CH_2)	1′α	0.94 (*t*, *J* = 6.0 Hz)	29.6 (CH_2)	1′α	0.98 (*t*, *J* = 6.0 Hz)
–	–	1′β	1.33 (*dd*, *J* = 6.5, 7.5 Hz)	–	1′β	1.14 (*d*, *J* = 7.0 Hz)	–	1′β	1.12 (*m*)
C-2′	24.2 (CH_2)	2′H	1.86 (*m*)	35.6 (CH_2)	2′H	1.18 (*m*)	33.1 (CH_2)	2′H	1.16 (*dd*, *J* = 6.0, 7.0 Hz)
C-3′	124.7 (CH)	3′H	4.96 (*t*, *J* = 7.0 Hz)	30.5 (CH)	3′H	1.41 (*h*, *J* = 1.6 Hz)	31.5 (CH)	3′H	1.36 (*h*, *J* = 6.0 Hz)
C-4′	130.7 (C)	–	–	23.1 (CH_3)	H_3-4′	1.03 (*d*, *J* = 5.0 Hz)	23.2 (CH_3)	H_3-4′	1.05 (*m*)
C-5′	25.3 (CH_3)	H_3-5′	1.62 (*s*)	–	–	–	–	–	–
C-6′	–	–	–	–	–	–	–	–	–
C-1″	16.7 (CH_3)	H_3-1″	1.65 (*s*)	15.6 (CH_3)	H_3-1″	1.80 (*s*)	17.4 (CH_3)	H_3-1″	1.76 (*s*)
C-2″	26.4 (CH_3)	H_3-2″	1.05 (*s*)	25.2 (CH_3)	H_3-2″	1.08 (*s*)	25.1 (CH_3)	H_3-2″	0.81 (*s*)
C-3″	27.9 (CH_3)	H_3-3″	1.09 (*s*)	21.9 (CH_3)	H_3-3″	0.86 (*s*)	21.3 (CH_3)	H_3-3″	0.91 (*s*)
C-4″	18.7 (CH_3)	H_3-4″	1.59 (*s*)	22.5 (CH_3)	H_3-4″	0.98 (*s*)	22.9 (CH_3)	H_3-4″	1.01 (*s*)
C-5″	–	–	–	23.1 (CH_3)	H_3-5″	1.03 (*d*, *J* = 5.0 Hz)	23.2 (CH_3)	H_3-5″	1.05 (*m*)

C. No. signifies carbon atom number.

[a] NMR spectra recorded using Bruker DPX 300 and AVANCE 300 MHz spectrometers.

[b] Values in ppm, multiplicity and coupling constants (*J* = Hz) are indicated in parentheses. Assignment were made with the aid of the ^{1}H–^{1}H–COSY, HMQC, and HMBC experiments.

Table 1B
NMR spectroscopic data of **4**–**5** in $CDCl_3$[a]

C. No.	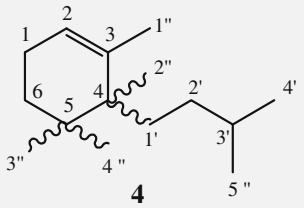 **4**			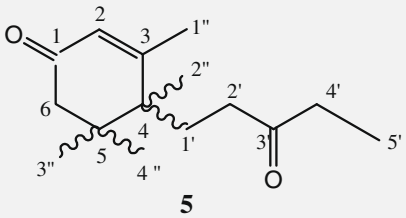 **5**		
	δ^{13}C NMR[b] (DEPT)	H	δ ^{1}H NMR (ppm)	δ^{13}C NMR[b] (DEPT)	H	δ ^{1}H NMR (ppm)
C-1	23.1 (CH_2)	1α	1.86 (*m*)	196.2 (C=O)	–	–
		1β	2.05 (*m*)			
C-2	122.8 (CH)	2H	5.16 (*t*, *J* = 5.6 Hz)	120.6 (CH)	2H	5.69 (*s*)
C-3	141.2 (C)	–	–	152.4 (C)	–	–
	–	–	–	–	–	–
C-4	48.1 (C)	–	–	53.2 (C)	–	–
	–	–	–	–	–	–
C-5	54.2 (C)	–	–	56.2 (C)	–	–
C-6	35.8 (CH_2)	6α	1.59 (*t*, *J* = 4.8 Hz)	48.7 (CH_2)	6α	2.30 (*d*, *J* = 4.5 Hz)
	–	6β	1.41 (*d*, *J* = 6.0 Hz)	–	6β	2.48 (*d*, *J* = 6.5 Hz)
C-1′	28.6 (CH_2)	1′α	0.87 (*t*, *J* = 6.0 Hz)	23.5 (CH_2)	1′α	1.20 (*t*, *J* = 6.5 Hz)
	–	1′β	0.98 (*m*)	–	1′β	1.36 (*d*, *J* = 4.8 Hz)
C-2′	35.3 (CH_2)	2′H	1.07 (*dd*, *J* = 6.5, 7.5 Hz)	38.4 (CH_2)	2′H	2.12 (*t*, *J* = 1.5 Hz)
C-3′	30.7 (CH)	3′H	1.32 (*h*, *J* = 2.0 Hz)	209.8 (C=O)	–	–
C-4′	22.7 (CH_3)	H_3-4′	0.93 (*d*, *J* = 4.6 Hz)	36.3 (CH_2)	4′H	2.42 (*q*, *J* = 7.0 Hz)
C-5′	–	–	–	7.3 (CH_3)	H_3-5′	1.98 (*t*, *J* = 7.0 Hz)
C-1″	21.7 (CH_3)	H_3-1″	1.71 (*s*)	18.3 (CH_3)	H_3-1″	1.79 (*s*)
C-2″	25.4 (CH_3)	H_3-2″	0.81 (*s*)	25.7 (CH_3)	H_3-2″	1.88 (*s*)
C-3″	22.3 (CH_3)	H_3-3″	1.02 (*s*)	20.8 (CH_3)	H_3-3″	1.12 (*s*)
C-4″	23.7 (CH_3)	H_3-4″	1.14 (*s*)	22.1 (CH_3)	H_3-4″	1.18 (*s*)
C-5″	22.7 (CH_3)	H_3-5″	0.93 (*d*, *J* = 4.6 Hz)	–	–	–

The notations are as indicated under Table 1.

*2.4.5. 3, 4, 5, 5-Tetramethyl-4-(3′-oxopentyl)-2-cyclohexen-1-one (**5**)*

Yellowish oil; Yield (% dw basis of alga) 2.0×10^{-3}; TLC R_f: 0.33 (*n*-hexane:EtOAc 4:1, v/v); GC retention time: 11.18 min.; elemental analysis found: C, 76.30; H, 10.31; O, 13.56 ($C_{15}H_{24}O_2$ requires C, 76.23; H, 10.24; O, 13.54); UV (CH_3OH), λ_{max} 256, 315 nm; IR ν_{max} (KBr): 3550 (–OH), 1258 (C–O), 3300 (as. C=O str.), 1715 (C=O ester str.), 1675 (amide I band, C=O str.), 1660, 1630, 942 (olefinic moiety); ^{1}H ($CDCl_3$, 300 MHz, δ ppm) and ^{13}C NMR ($CDCl_3$, δ ppm) data, see Table 1B; EIMS *m*/*z* (rel. int.%) 236 [M^+] (31); 168 (22), 140 (19), 112 (100), 100 (56); HRMS (ESI): calcd. for $C_{15}H_{24}O_2$ 236.3489, found 236.3509.

2.5. Antioxidant assay using scavenging effect of crude solvent extracts and purified compounds on 1,1-diphenyl-2-picryhydrazyl (DPPH.) free-radicals

Free-radical-scavenging capacity of the solvent extracts of *Ulva fasciata* and the purified compounds were tested by bleaching of the stable 1,1-diphenyl-2-picrylhydrazyl (DPPH) using the method proposed by Shimada, Fujikawa, Yahara, and Nakamura (1992). Briefly, the solvent extracts at different concentrations (3 ml, 10–100 μg/ml) were added to the solution of DPPH (0.5 ml, 0.2 mM in 95% EtOH); the mixture was shaken vigorously, and allowed to stand at room temperature for 30 min. The absorbance was measured at 517 nm by using a UV–visible spectrophotometer (Varian Cary UV-100). Lower absorbance of the reaction mixture indicated higher free-radical-scavenging activity. Percentage inhibition was calculated by the following formula:

$$\text{DPPH radical scavenging effect } (\%) = [(A_0 - A_1)/A_0] \times 100$$

where A_0 was the absorbance of the control and A_1 was the absorbance in the presence of the standard or solvent extracts.

To assay the scavenging activities of the purified compounds, five dilutions of both test and standard solutions in methanol were prepared with the following final concentrations of each substance: 10, 5, 2.5, 1.25 and 0.625 mM. Stock solutions of two known antioxidants (BHT and gallic acid) were also prepared. Cinnamic acid was used as a negative control. For the tests, methanolic solutions of standards and each purified compound at various concentrations (50 ml, 0.625–10 mM) were added to test tubes containing a fresh solution of DPPH (100 ml, 30 mM) in MeOH (0.6 ml). MeOH (100 ml) in test tubes was used as a blank, and 100 mM solutions (100 ml) of DPPH as controls. The scavenging activity on the DPPH radical was expressed as IC_{50}, which is the concentration of the test solution required to give a 50% reduction in the absorbance from that of the control solution.

2.6. 2,2′-Azino-bis (3-ethylbenzthiazoline-6-sulfonate) (ABTS) radical cation decolorisation assay

The ABTS assay was also employed to measure the antioxidant activity of the crude solvent extracts and purified compounds (Nenadis, Wang, Tsimidou, & Zhang, 2004; Ozgen, Reese, Tulio, Scheerens, & Miller, 2006; Re et al., 1999). Briefly, a stock solution of ABTS radical cation was prepared by dissolving ABTS (7 mM, 5 ml in deionised water) with potassium persulfate (14.7 mM, 1 ml). The reaction mixture was left to stand at room temperature overnight (16 h) in the dark. The intensely-coloured $ABTS^{\cdot+}$ radical cation was diluted with EtOH to an absorbance of about 0.70 at 734 nm. The decolorisation assay was started by mixing the diluted ABTS solution (2 ml) with different solvent extracts (20 μl, 20–100 μg/ml) and the test compounds (10–50 μM). Test compounds were dissolved with dimethylsulfoxide (10% DMSO) before analyses. At 4 min after mixing, the absorbance was measured at 734 nm. Controls without $ABTS^{\cdot+}$ were used to allow

for any absorbance of the extracts themselves. In a control experiment, a test compound solution was replaced with DMSO (10%), and the radical-scavenging activities of the crude extracts and test compounds were expressed as a percentage inhibition based on absorbance. Fresh stocks of $ABTS^{\cdot+}$ solution were prepared every five days due to self-degradation of the radical. Trolox, the water-soluble α-tocopherol analogue served as a standard in this study.

2.7. Statistical analysis

Results were analyzed using one-way analysis of variance (SPSS, Version 10.0). A significance level of 95% ($p = 0.05$) was used throughout, and significant differences among different treatments were determined by post hoc measurements. All measurements were performed in triplicate ($n = 3$), and the values were expressed as means of three replicate determinations.

3. Results and discussion

3.1. Free-radical-scavenging activities of the crude solvent extracts of Ulva fasciata

The 1,1-diphenyl-2-picrylhydrazyl (DPPH) and 2,2′-azino-bis(3-ethylbenzthiazoline-6-sulfonate) ($ABTS^{\cdot+}$) radical-scavenging activities of the crude solvent extracts from *Ulva fasciata* Delile are shown in Fig. 1. Fig. 1 illustrates a decrease in the concentration of $DPPH^{\cdot}$ radical due to the scavenging ability of the crude extracts. The scavenging effect of the solvent extracts tested at 50 μg/ml on the DPPH radical decreased in the order of EtOAc > CH_2Cl_2 > *n*-hexane, and were 69.7%, 53%, and 22.3%, respectively. The free-radical-scavenging activities of EtOAc and CH_2Cl_2 fractions increased with increasing concentration. However, the effects of EtOAc extracts at higher concentration (0.1 mg/ml) reached a plateau (Fig. 1).

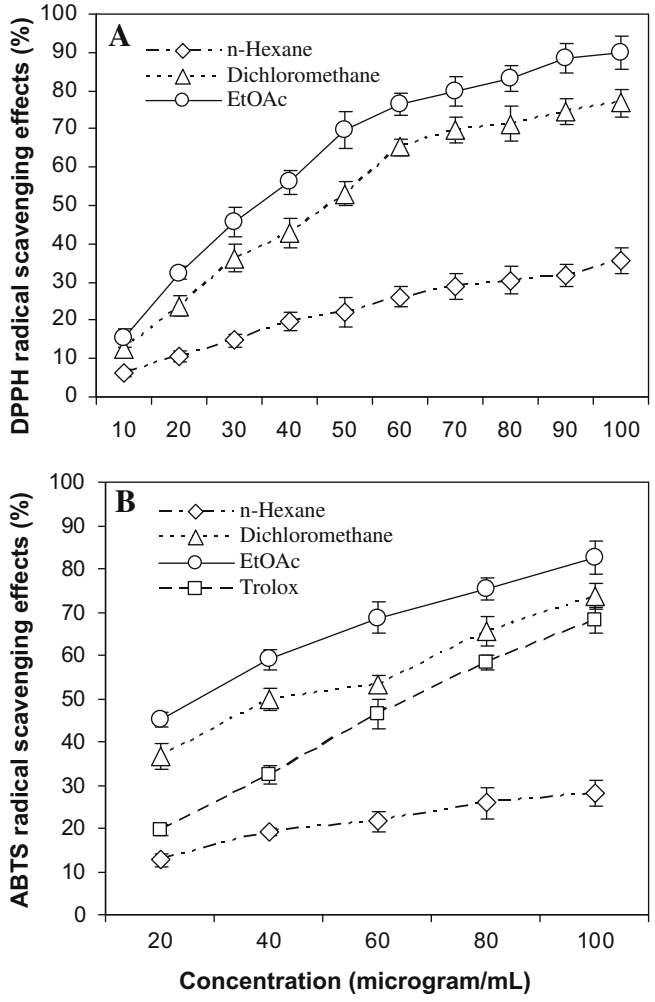

Fig. 1. Free-radical-scavenging activities of different concentrations of solvent extracts (10–100 μg/ml) on (A) $DPPH^{\cdot}$ and (B) $ABTS^{\cdot+}$ radical.

The results were found to be similar for the $ABTS^{\cdot+}$ radical-scavenging activities of the crude solvent extracts. A significant ($p = 0.05$) decrease in the concentration of $ABTS^{\cdot+}$ was observed due to the scavenging ability of the EtOAc and CH_2Cl_2 extracts from *U. fasciata*. An 82.6% radical-scavenging activity was apparent by EtOAc extract at 0.1 mg/ml, whereas the CH_2Cl_2 extract exhibited a 73.5% inhibition of activity at the same concentration. The *n*-hexane extracts exhibited lowest radical-scavenging activity (28.1% at 0.1 mg/ml; Fig. 1). Based on the data obtained from this study, EtOAc extract was found to be the most powerful free radical scavenger, which was further fractionated chromatographically to purify the active antioxidant compounds as illustrated in the following section.

3.2. Chromatographic purification and spectral analyses of sesquiterpenoid derivatives from Ulva fasciata

Chromatographic separation led to the isolation of five sesquiterpenoids (**1**–**5**) *viz*., 2,5,5-trimethyl-4-(4′-methyl-3′-pentenyl)-2-cyclohexen-1-ol (**1**) (1.4×10^{-3}% dw), 4-isopentyl-3,4,5,5-tetramethyl-2-cyclohexen-1-ol (**2**) (1.7×10^{-3}% dw), and 4-isopentyl-3,4,5,5-tetramethyl-2-cyclohexen-1-ol (**3**) (0.8×10^{-3}% dw), 6-isopentyl-1, 5, 5, 6-tetramethyl-1-cyclohexene (**4**) (1.1×10^{-3}% dw), and 3,4,5,5-tetramethyl-4-(3′-oxopentyl)-2-cyclohexen-1-one (**5**) (2.0×10^{-3}% dw) (Tables 1A and 1B). The molecular structures of the purified compounds were proposed on the basis of comprehensive analysis of the ^1H NMR, ^{13}C NMR, including 2D-NMR experiments (^1H–^1H–COSY, HMQC, HMBC, and NOESY), and mass spectra.

3.2.1. 2,5,5-Trimethyl-4-(4′-methyl-3′-pentenyl)-2-cyclohexen-1-ol (*1*)

Compound **1** was isolated as yellowish oil upon repeated column chromatography using silica gel as adsorbent. Its mass spectrum exhibited a molecular ion peak at *m*/*z* 222, which in combination with its ^1H and ^{13}C NMR data (Table 1A) led to the molecular formula $C_{15}H_{26}O$, with three degrees of unsaturation. HRMS analysis furnished the molecular weight as 222.3672. The IR spectrum exhibited absorption bands corresponding to hydroxyl groups (3040 cm^{-1}) and olefinic system (1461 cm^{-1}, 1035 cm^{-1}, 820 cm^{-1}). The ^1H NMR spectrum indicated the presence of three methyl singlets (δ 1.65, δ 1.59, and δ 1.62 assigned as H_3-1″, H_3-4″, and H-5′, respectively), two olefinic (δ 5.33, *d*; δ 4.96, *t*), and one aliphatic methine signal (δ 3.89, *t*) (Table 1A). The downfield shift of olefinic methine at δ 5.33 indicated its vicinity to a electronegative group. The aliphatic methine singlet at δ 3.89 assigned to be *vicinal* to the carbon atom attached with the electronegative hydroxyl group (δ 2.30, *bs*). D_2O exchange apparently confirmed the hydroxyl signal at δ 2.30. The downfield appearance of the aliphatic methylene signals at δ 1.53 (*m*) and δ 1.76 (*d*, $J = 6.8$ Hz) indicated their close vicinity to a electronegative group (Table 1A). The multiplicity of carbon atoms was determined using ^{13}C NMR including DEPT experiments, which revealed the presence of five methyl groups, three methylene groups, three methine groups and three quaternary carbons, indicating the presence of 26 hydrogen atoms connected to fifteen carbon atoms consistent with a sesquiterpene skeleton (Fig. 2A). The ^{13}C NMR spectrum

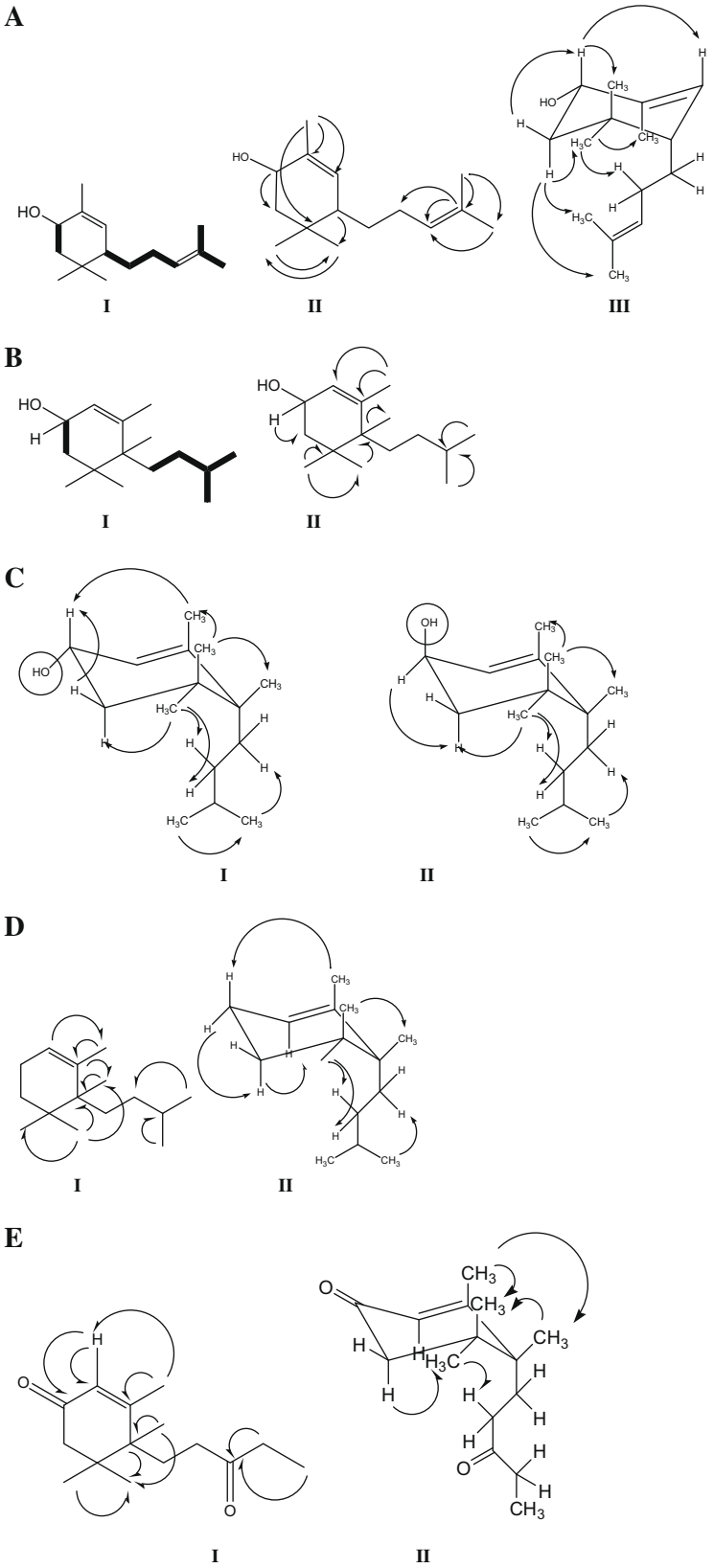

Fig. 2. 2D-NMR correlations of the purified sesquiterpenoids. (A) 2D-NMR correlations of 2,5,5-trimethyl-4-(4′-methyl-3′-pentenyl)-2-cyclohexen-1-ol (**1**). I: Key ^{1}H–^{1}H–COSY couplings (bold face bonds); II: HMBC couplings; III: Key NOESY correlations. (B) 2D-NMR correlations as observed in 4-isopentyl-3,4,5,5-tetramethyl-2-cyclohexen-1-ol (**2**). I: Key ^{1}H–^{1}H–COSY couplings (bold face bonds); II: Key HMBC couplings (single barbed arrows); (C) Comparison of key NOESY correlations (indicated as arrows) between compounds **2** and **3**. I: The hydroxyl group in **2** is equatorial resulting in long range coupling of β-H at C-6 with CH_3 at 3rd carbon of the alicyclic ring. II: In compound **3**, the axially oriented α-H atom was found to exhibit NOE couplings with C-6 hydrogen and side chain protons. (D) 2D-NMR correlations as observed in 6-isopentyl-1,5,5,6-tetramethyl-1-cyclohexene (**4**). I: Key HMBC couplings (single barbed arrows). II: Key NOESY correlations (double barbed arrows). (E) 2D-NMR correlations in 3,4,5,5-tetramethyl-4-(3′-oxopentyl)-2-cyclohexen-1-one (**5**). I: Key HMBC couplings (single barbed arrows). II: Key NOESY correlations (double barbed arrows).

displayed signals characteristic of double bond at δ 124.7 and δ 130.7, assigned as C-3′ and C-4′, respectively, and also at δ 132.4 (assigned to be C-2) and δ 126.1 (assigned to be C-3). The downfield shift of the methine signal at δ 70.2 (CH) indicated its vicinity to an electronegative group. This indicates that the carbon may be linked to an α-OH resulting in resonance at slightly downfield. The connectivity within the molecule was established by interpretation of the ^{1}H–^{1}H–COSY and HMBC spectra. In ^{1}H–^{1}H–COSY spectrum, several key couplings indicating a sesquiterpene skeleton was apparent (Bombarda et al., 2001; Faraldos, Wu, Chappell, & Coates, 2007). In the HMBC spectrum, key couplings were observed that substantiated the connectivity found in ^{1}H–^{1}H–COSY (Fig. 2A). Two of the methyl groups at δ 18.7 (assigned to be C-4″) and δ 25.3 (assigned to be C-5′) were found to correlate with each other, as well as with protons at δ 1.86 (at C-2′) as evident from the HMBC spectrum (Fig. 2A). The methyl singlets at δ 1.59 and δ 1.62, and the methine (at δ 4.96) were coupled to the olefinic quaternary carbon at δ 130.7 (assigned to be as C-4′); suggesting that these two methyl groups were *geminal* and connected to C-4′, which in turn was found to be connected to an olefinic methine carbon (assigned to be as C-3′). The carbon atom at δ 130.7 (assigned to be as C-4′) exhibited HMBC coupling to δ 1.86 (assigned to be as H-2′) that in the ^{1}H–^{1}H–COSY showed coupling to δ 1.21 (*t*) as well as to δ 4.96 (*t*) assigned to be as H-3′ (Fig. 2A). The protons at δ 1.33 (*dd*) were found to exhibit strong ^{1}H–^{1}H–COSY coupling with the proton at δ 1.82 (*t*), and also with the proton at δ 4.96 (*t*), which indicate the presence of a propylenic moiety. The HMQC, ^{1}H–^{1}H–COSY, and HMBC couplings apparently constitute the 2-methylhex-2-ene moiety of **1**. The methyl at H_3-1″ (δ 1.65, *s*) was found to be coupled to each of olefinic quaternary (δ 132.4) and methine carbons (δ 126.1) as evident from the HMBC spectrum (Fig. 2A). The quaternary carbon at δ 30.9 exhibited coupling to olefinic methyl singlet at δ 1.65 (H_3-1″), which itself exhibited coupling to δ 132.4 and δ 126.1. The proton at δ 3.89 (*t*) exhibited ^{1}H–^{1}H–COSY correlations with proton at δ 1.76 (*d*). HMBC correlations between δ 1.65 (*s*)/δ 132.4 (C)/δ 30.9 (C), δ 1.05 (*s*)/δ 30.9 (C), δ 1.09 (*s*)/δ 30.9 (C), and δ 1.05 (*s*)/δ 26.4 (CH_3) assigned the positions of methyl groups in an olefinic ring skeleton. Two of the primary methyl groups at δ 26.4 (C-2″ and C-3″) were found to be *geminal* as indicated by couplings between the two groups in the HMBC spectrum (Fig. 2). The signal at δ 70.2 was assigned to be a tertiary carbon bonded to a hydroxyl group. The position of the hydroxyl group at C-1 (δ 2.30, *bs*) was confirmed by the HMBC correlations of the protons. The tertiary alcohol also deduced to be at C-1 as observed from the couplings between δ 70.2 (C-1), the methylene protons at δ 1.53 (C-6), and the olefinic methine proton at δ 126.1 (C-3). The trimethyl cyclohexenol moiety was assigned based on the HMQC and HMBC correlations of the carbon and proton atoms. The relative stereochemistries of the chiral centers were deduced from the NOESY spectrum and *J*-values. Significant NOE correlations were apparent between δ 3.89 (H-1)/ δ 1.82 (H-4) indicating that H-1 and H-4 are on the same side of **1**. The axial configuration of H-1 and H-4 were indicated from their coupling constant (J = 6.8 Hz). NOE correlations were apparent between δ 2.30 (1_α-OH)/δ 1.21 (H_α-1′)/δ 1.53 (H_α-6) that indicate their close proximity and α-disposition. NOE correlations between δ 5.33 (H-3)/δ 3.89 (H-1)/δ 1.05 (H_3-2″), and δ 1.82 (H-4)/δ 3.89 (H-1) indicated the close proximity of these groups and their β-disposition. The spectral interpretations infer the planar structure of **1** as 2,5,5-trimethyl-4-(4′-methyl-3′-pentenyl)-2-cyclohexen-1-ol.

3.2.2. 4-Isopentyl-3,4,5,5-tetramethyl-2-cyclohexen-1-ol (**2**)

Compound **2**, which was isolated as a yellow oil has the molecular formula $C_{15}H_{28}O$, and molecular weight of 224.3845, as shown by HRMS analysis. The ^{1}H NMR spectra revealed the signals of olefinic double bond (δ 5.31, *d*), and a hydroxyl function (δ 4.21, *bs*). The hydroxyl group was further confirmed by D_2O-exchange reactions. The presence of six methyl signals along with three each of methylene and methine protons in the ^{1}H NMR spectra were consistent with a sesquiterpene skeleton (Bombarda et al., 2001), which was further supported by ^{13}C NMR-DEPT data (Table 1A). The downfield shift of the olefinic methine group at δ 5.31 (*d*) indicated its close vicinity to the hydroxyl group. The methine proton at δ 3.89 (*dd*) and aliphatic methylene protons at δ 1.52 and δ 1.73 observed downfield shift apparently due to their vicinity towards a hydroxyl group. The ^{13}C NMR spectrum exhibited signals typical of olefinic double bond at δ 123.8 (CH) and δ 140.2 (C). The methine signal at δ 68.4 and methylene signal at δ 44.3 indicated their vicinity to an electronegative group. It is apparent that the carbon linked to α-OH usually exhibits the NMR resonance at lower magnetic field than the β-OH principally because of inductive effect. All protonated carbons and their protons were matched precisely by ^{1}H–^{1}H–COSY and HMQC experiments, and comparison with literature data (Bombarda et al., 2001). Diagnostic ^{1}H–^{1}H–COSY correlations were apparent between the proton at δ 3.89 (assigned as carbinolic proton), and both the olefinic proton (at δ 5.31) and the methylene protons (δ 1.52, 1.73) (Fig. 2B). The multiplicity and downfield shift of the aliphatic methine proton at δ 1.41 (*h*) and its ^{1}H–^{1}H–COSY correlation with the magnetically equivalent methyl protons at δ 1.03 (*d*) indicated the presence of an isopropyl group in **2**. ^{1}H–^{1}H–COSY correlations were apparent between δ 1.03 (*d*) and δ 1.41 (*h*) (assigned as isopropyl methine proton) that in turn exhibited correlations with methylenic protons at δ 1.18 (*m*) and δ 1.14 (*d*). HMQC correlations between primary carbon at δ 2.31 and tertiary carbon atom at δ 30.5 also indicated the isopropyl moiety in **2**. The latter was found to exhibit HMQC correlation with the secondary carbons (at δ 35.6 and δ 28.2) thus indicating the presence of an isobutyl moiety in **2**. The HMBC spectrum exhibited correlations between δ 68.4 with olefinic methine proton at δ 5.31 (*d*) and methylene protons at δ 1.52 (*d*) and δ 1.73 (*d*) (Fig. 2B). HMBC correlations were also apparent between quaternary carbon atom at δ 52.9 and methyl protons at δ 0.86 (*s*). The HMBC long-range correlations were observed between methyl carbon δ 21.9 and methyl protons at δ 0.86. The methyl protons exhibited HMBC correlation with the quaternary carbon atom at δ 57.1, and methine carbon at δ 52.9, which in turn correlated with methylene protons at δ 0.94 (*t*) and δ 1.14 (*d*). These correlations along with HMQC experiment indicated that there are *geminal* dimethyl groups at C-5 position, and are the parts of the ring skeleton having an olefinic moiety. The HMBC correlations were apparent between methine carbon atom at δ 30.5 and methyl protons at δ 1.03 (*d*). The former (δ 30.5) also exhibits HMBC correlation with methylene protons at δ 1.18 (*m*) and δ 1.14 (*d*), which indicate the presence of isobutyl moiety in **2**. The best strategy for the determination of relative stereochemistry by NMR spectroscopy is to rely on H-H coupling constants that provide information on NOE-derived spatial relationships. The large value to the coupling constant (J = 7.5 Hz) observed for H_β-6 indicated its axial position. In the NOE spectrum, a strong correlation between H_β-6 (δ 1.73) and H_β-1 (δ 3.89)/H_3-2″ (δ 1.08) was observed, positioning the C-4 methyl group at the axial position. A strong NOE between H_3-3″ (δ 0.86)/H_α-1′ (δ 0.94) was in agreement with the methyl and methylene groups being in the equatorial position (Fig. 2C). A diagnostic positive NOE effect was observed between δ 1.52 (*d*, J = 5.6 Hz) and δ 0.86, indicating that both H_α-6 and H_3-3″ were in similar orientation (Fig. 2C). The relative stereochemistries of the methyl groups at C-3 and C-4 were suggested to be *cis* by comparison of the ^{13}C chemical shift of H_3-1′ (δ 15.6), and H_3-2″ (δ 25.2). The β-configuration of the methyl protons at δ 1.08 (H_3-2″) at C-4 was deduced from the NOE correlations between H-1 (δ 3.89) and H_3-2″ (δ 1.08). This results confirmed that hydroxyl group at C-1 (δ 4.21) is α-oriented and equatorially disposed.

NOE correlations between OH-1 and H-6 (δ 1.52)/H_3-3″ (δ 0.86) inferred that they were equatorially oriented (Fig. 2C). The $-H_\beta$ group at C-1 exhibited a downfield shift (δ 3.89) apparently because of the *vicinal* hydroxyl group. All proton and carbon assignments were reported in Table 1A, which were in conformity with 4-isopentyl-3,4,5,5-tetramethyl-2-cyclohexen-1-ol (**2**).

3.2.3. 4-Isopentyl-3,4,5,5-tetramethyl-2-cyclohexen-1-ol (**3**)

The IR spectrum of **3** revealed prominent absorption band at ν_{max} 3500 cm^{-1}, attributed to hydroxyl functionality. Its mass spectrum exhibited a molecular ion peak at *m/z* 224, which in combination with ^1H and ^{13}C NMR data led to the molecular formula of $C_{15}H_{28}O$ with two double bond equivalents. HRMS analysis revealed the molecular weight as 224.3836. The ^1H spectra indicated the presence of six methyl groups and one double bond (δ_H 4.92, *d*). The DEPT-^{13}C NMR spectrum exhibited signals for all the 15 carbons (Table 1A). The downfield shift of the methine carbon (δ_C 64.1) indicated its vicinity to an electronegative group. However, the chemical shift of –CH carbon apparently linked to an –OH group was recorded at slightly upfield (δ_C 64.1) as compared to that in **2** (δ_C 68.4). This can be explained by the fact that the carbon (C-1) linked to α-OH (as in **2**) usually exhibits NMR resonance at slightly lower magnetic field than β-OH, primarily due to inductive effect. Other signals are similar to those of **2**, and therefore indicated their structural similarity. The ^1H–^1H–COSY correlations between H-1 (δ 3.92) with H-2 (δ 4.92) and H_2-6 (δ H_a = 1.50, δ H_b = 1.52) indicated that the carbinolic carbon was linked with the olefinic carbon atom. HMBC long-range correlations between H-2 (δ 4.92) with C-2 (δ 123.6), C-3 (δ_C 140.7), and C-5 (δ 56.5); H_3-2″ (δ 0.81) with C-4 (δ_C 51.3) and C-3 (δ 140.7); H-1 (δ_H 3.92) with C-1 (δ_C 64.1) and C-6 (δ_C 43.7) suggested the methyl-substituted cyclohexene ring skeleton as in **2**. A pronounced NOESY correlation between –OH group (δ 4.08) and H_3-2″ (δ 0.81) was consistent with their *cis* orientation on the top face of the molecule. Pronounced NOE correlations were apparent between H-1 (δ 3.92) with H_α-1′ (δ 0.98) and H_3-5″ (δ 1.05), which in turn was found to correlate with H_2-2′ (δ 1.16). These results indicated the *cis*-orientation of these groups at the down face of **3**. Other NOE correlations are comparable with that of **2**, the only difference being the –OH group is β-oriented, and exhibited NOE correlation with H_3-2′ unlike **2**, where the –OH group is α-oriented and does not show correlation with H_3-2′. Comparison of NOE correlation between **2** and **3** concluded that the hydroxyl group in **2** is equatorially oriented resulting in long range NOE-couplings of H_β- at C-1 with the $-CH_3$ group located at C-4 of the alicyclic ring. In **3**, the axially oriented H_α atom at C-4 was found to exhibit NOE-couplings with C-1 hydrogen atom and side chain aliphatic protons. Analysis of carbon values of the cyclohexene ring of both compounds further supported this suggestion. Based upon these interpretations, the compound was deduced to be as 4-isopentyl-3,4,5,5-tetramethyl-2-cyclohexen-1-ol (**3**).

3.2.4. 6-Isopentyl-1,5,5,6-tetramethyl-1-cyclohexene (**4**)

The ^1H NMR spectrum of 6-isopentyl-1,5,5,6-tetramethyl-1-cyclohexene (**4**) showed that the singlet methyl at C-2″ (δ 25.4) was positioned at the ring junction like **2** and **3**. Assignment of different resonant peaks to the respective carbon atoms are presented in Table 1B. The other spectral assignments are similar to that of **3** excepting the upfield shift of C-3 and C-4 protons apparently due to the absence of any electronegative moiety (-OH group) (Fig. 2D). The key HMBC and NOE correlations of 4 have been illustrated in Fig. 2D.

3.2.5. 3,4,5,5-tetramethyl-4-(3′-oxopentyl)-2-cyclohexen-1-one (5)

Compound **5**, which was isolated as a yellowish oil, has the molecular weight of 236.3509, and molecular formula of $C_{15}H_{24}O_2$ as determined by the analysis of HRMS and NMR spectral data. A conjugated α,β-unsaturated carbonyl system was apparent from the UV-spectra. The presence of the carbonyl group was established by a strong absorption band in IR spectrometry (1715 cm^{-1}) and ^{13}C NMR spectrum (Table 1B). The downfield shift of the protons at δ 2.30 (*d*) and δ 2.48 (*d*) indicated the presence of an electronegative group (>C=O) in their close vicinity. The methylene carbons exhibited downfield shifts, thereby further indicating the presence of a C=O group adjacent to the carbon atom holding the downfield protons. The multiplicity and downfield shift of the protons at δ 1.98 (*t*) and δ 2.42 (*q*) indicated the ethyl functionality attached with a carbonyl group. This was supported by the downfield shift of the secondary carbon atom at δ 36.3 ($-CH_2-$) in ^{13}C NMR spectrum. The ^{13}C NMR spectra exhibited signals of two carbonyl groups (δ 196.2 and 209.8) and olefinic double bond (δ 152.4 and 120.6).

The nuclear structure of cyclohexenone in **5** was deduced based on the data in published literature (Guo et al., 2009; Rezanka, Dembitsky, & Hanus, 2003; Taylor & Jacobsen, 2006). The methylene carbon atom at δ 38.4 (CH_2) exhibited downfield shift, apparently due to the carbonyl group at δ 209.8. HMQC correlations between δ 7.3 (CH_3)/δ 2.42 (*q*), δ 36.3 (CH_2)/δ 1.98 (*t*), δ 209.8 (C=O)/δ 2.42 (*q*), δ 209.8 (C=O)/δ 2.12 (*t*), δ 38.4 (CH_2)/δ 1.20 (*t*), and δ 23.5 (CH_2)/δ 2.12 (*t*) indicated the presence of a 3-pentanone moiety in **5**. ^1H–^1H–COSY correlations were apparent between δ 1.20 (*t*) and δ 2.12 (*t*). A very strong HMBC correlation between δ 196.2 (assigned as C=O group) and the carbon atom at δ 5.69 (*s*) indicated their adjacent position. Correlations between δ 1.79 (assigned to be as H_3-1″), H-2, and H_α-6 with δ 196.2 (>C=O) as in the HMBC spectrum led to the assignment of the ketone to C-1 (Fig. 2E). HMQC correlations between δ 196.2 (C=O)/δ 5.69 (olefinic)/δ 2.48 (*s*) indicated the presence of a $-CH-(C=O)-CH_2-$ group in **5** (Fig. 2E). This was further supported by the HMQC spectrum where strong correlations were apparent between carbon at δ 120.6 (CH), carbonyl group at δ 196.2, and secondary carbon at δ 48.7 with δ 2.48 (*d*) and δ 5.69 (*s*). These observations indicated the presence of $=CH-C(=O)-CH_2-$ moiety. HMQC correlations were also apparent between the carbon atoms at δ 152.4/δ 5.69 (*s*), δ 53.2 (C)/δ 1.20 (*t*), and δ 56.2 (C)/ δ 2.48 (*d*). In general, the secondary carbon appears between δ 20 and 30 ppm when electronegative groups are not either linked to it or present in the vicinity. However, in the present case though the C-6 carbon atom is not directly linked with oxygen atom in compound **5**, it dwells in a close vicinity to the >C=O group, and therefore exhibited a slight downfield shift (δ 48.7) as compared to the reference secondary carbon atom (δ 20–30). The H-6 methylene protons are "pseudo-homotopic" and attached with one parent carbon atom (i.e., *geminal* protons), and therefore ideally the protons should exhibit only one chemical shift value. However, since one of the protons (6H-β) shares the identical plane with that of the carbonyl (>C=O), the same exhibits downfield shift (δ 2.48 ppm) relative to the other (6-Hα, δ 2.30 ppm). The presence of a cyclohexenone moiety was thus deduced based upon these observations and data in published literature (Guo et al., 2009; Taylor & Jacobsen, 2006). Since the HMBC spectrum exhibited correlations between δ 2.48, δ 5.69, δ 1.88 to the carbon atom at δ 56.2 (C), it was assigned to be as C-5 carrying the *geminal* dimethyl groups. HMQC correlations were apparent between δ 1.88 (*s*) and quaternary carbon atom at δ 53.2 (C), which in turn exhibited correlation with δ 1.20 (*t*) and δ 1.36 (*d*). HMBC correlations between δ 1.88 (*s*) and quaternary and secondary carbons at δ 53.2 (C) and δ 23.5 (CH), respectively, indicated that the side chain containing 3-pentanone moiety was linked with the quaternary carbon atom at δ 53.2 (Fig. 2E). The strong correlation of protons at δ 1.12 (*s*) with protons at δ 1.88 (*s*) and δ 2.48 (*d*) in the NOESY spectrum provided evidence for the β-configuration of these protons (Fig. 2E). Based upon these interpretations and

Table 2
In vitro antioxidant activity of isolated compounds (**1**–**5**) from *Ulva fasciata*.

Compound number	Compound name	DPPH radical-scavenging activity (IC_{50}, mM)[c]
1	2,5,5-Trimethyl-4-(4-methylpent-3-enyl)-2-cyclohexen-1-ol	13.74 ± 1.38
2	4- Isopentyl-3,4,5,5-tetramethyl-2-cyclohexen-1-ol	23.60 ± 1.15
3	4-Isopentyl-3,4,5,5-tetramethyl-2-cyclohexen-1-ol	20.83 ± 0.92
4	6-Isopentyl-1,5,5,6-tetramethyl-1-cyclohexene	80.56 ± 2.43
5	3,4,5,5-Tetramethyl-4-(3-oxopentyl)-2-cyclohexene-1-one	10.24 ± 0.98
Controls	Gallic acid[a]	4.50 ± 0.31
	BHT[a]	11.93 ± 0.57
	Cinnamic acid[b]	96.35 ± 1.82
LSD ($p = 0.05$)		1.09

[a] Gallic acid and BHT were used as positive controls.
[b] Cinnamic acid was used as negative control.
[c] IC_{50} (mM) values were calculated from regression lines using different concentrations as detailed in Materials section. Values were expressed as means of three replicate determinations ± standard deviation.

comparison of data in the published literature the compound was deduced to be 3,4,5,5-tetramethyl-4-(3′-oxopentyl)-2-cyclohexen-1-one (**5**).

3.3. Free radical-scavenging activity of the purified compounds against DPPH radical

Antioxidants are defined as substances that when present at low concentrations, in relation to oxidisable substrates, inhibit oxidative processes, being oxidised themselves. The antioxidant activity (in terms of radical-scavenging capacity) of different sesquiterpenoids (**1**–**5**), as well as positive (BHT and gallic acid) and negative controls (cinnamic acid), were measured by monitoring the scavenging of the free radical DPPH. The DPPH radical is considered to be a model of a lipophilic radical in this study. In the presence of an antioxidant, this can donate an electron to DPPH radical, the purple colour typical of free DPPH radical decay (Fayaz et al., 2005). Thereafter the DPPH radical receives a proton from the antioxidant and becomes a protonated DPPH species. The change in absorbance at 517 nm is followed spectrophotometrically (Wu, Ho, Shieh, & Lu, 2005).

Antioxidant activities of the compounds were tested by measuring the IC_{50} values are summarised in Table 1A. The order of radical-scavenging ability of the test compounds was as follows: **5** > **1** > **2** > **3** > **4**. Compounds **5** and **1** exhibited effective antioxidant scavenging activity against DPPH radicals with IC_{50} values of 10.2 and 13.7 mM, respectively; gallic acid (IC_{50} = 4.5 mM) and BHT (IC_{50} = 11.9 mM) were used as positive controls. The radical-scavenging activity of **5** was that of BHT, a well-established synthetic antioxidant. Compound **5**, with two carbonyl groups and one olefinic group, exhibited the highest radical-scavenging capacity (IC_{50} = 10.2 mM), while **1** with only one –OH group showed a slightly weaker scavenging capacity (IC_{50} = 13.7 mM) (Table 2). Though **1** and **2** possessed equatorially oriented free hydroxyl groups, the bioactivity of the latter was found to be less, due to the extended olefinic side chain (2-methyl-2-pentene) in the former resulting in favourable interaction. Compound **3** has lower activity (IC_{50} = 20.8 mM) compared to that of **2** (IC_{50} = 23.6 mM) due to the fact that **3** has an α-oriented C-1 hydroxyl group in the 3,4,5,5-tetramethyl-2-cyclohex-2-en-l-ol moiety as compared to the unfavourable β-orientation in **2**, resulting in lowering in activity in the latter. Though structurally similar, **1** exhibited higher activity than compound **2** due to the presence of a $–CH_3$ group at C-2 position of the ring, which by virtue of its $^{+}$I-effect increases electron density on carbinolic oxygen atom thus increasing the chance of electron release from the molecule. The $^{+}$I-effect of a proton (at C-2 position of **2**) is lower than that of a $–CH_3$ group, resulting in lower electron density on C-1_{OH} atom and lower e^{-} and H^{+}-releasing capacity. The $–CH_3$ group at C-3 position of the ring has a lower effect in increasing electron density on C-1_{OH} atom as evident by the lower activity of **2** and **3** having $–CH_3$ group at C-3 position. These results indicated that the antioxidant activities appeared to be related to the number of protons available for donation by hydroxyl groups. This is further supported by the fact that non-hydroxylated sesquiterpene (**4**) exhibited the lowest activity (IC_{50} = 80.5 mM) among all the test molecules.

3.4. Determination of free-radical-scavenging activity by ABTS method

The antioxidant activities determined by the ABTS radical ion assay correlated highly with that of the DPPH radical assay. The

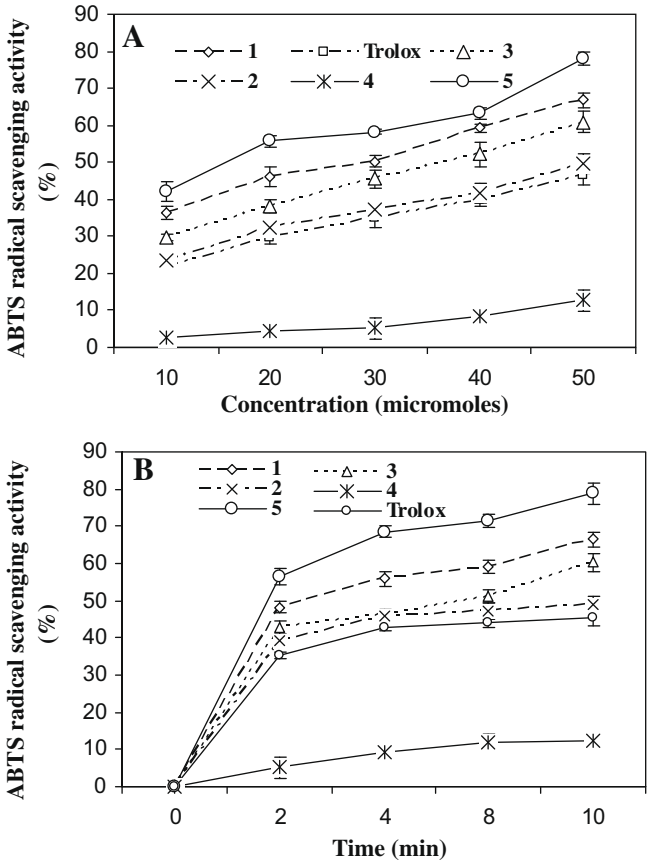

Fig. 3. ABTS+ radical cation-scavenging activities of 1–5 isolated from *Ulva fasciata* (A) $ABTS^{\cdot+}$ scavenging activity of 1–5. ABTS radical-scavenging activity was indicated as% inhibition. Each point represents mean ± S.E. of three separate experiments. (B) Time course of $ABTS^{\cdot+}$ scavenging in the presence of purified compounds (50 μM) relative to Trolox (α-tocopherol analogue).

ABTS scavenging activities of **1** and **3** were found to be about 1.4 and 1.3-fold higher than that of Trolox (Fig. 3A). However, the radical-scavenging activity of **1** was found to be weaker than that of **5**. Compound **5** exhibited 78 ± 1.9% $ABTS^{\cdot+}$ radical-scavenging activity tested at 50 μM, with 66.8 ± 1.5% scavenging activity by **1** at the same concentration (Fig. 3A). The scavenging effect of the compounds decreased with the order: **5** > **1** ≫ **3** > **2** ≫ **4** (Fig. 3A). The radical-scavenging effect was found to decrease with decreasing concentration. For example, a 59.2 ± 1.1% radical-scavenging effect was apparent by **1** at 40 μM, whereas 50.3 ± 1.6% inhibition of activity was recorded at 30 μM concentration (Fig. 3A). The compound without any hydroxyl group (**4**) exhibited the lowest $ABTS^{\cdot+}$ radical-scavenging activity (12.8 ± 2.9% at 50 μM), apparently due to a lack of hydrogen-donating ability. ABTS radical ion assay involves the oxidation of ABTS, a non-phenolic heterocyclic compound, to a coloured radical cation, $ABTS^{\cdot+}$ in the presence of free radicals (Re et al., 1999). The antioxidant activity of the molecules is based on the inhibition of $ABTS^{\cdot+}$ (Re et al., 1999). Fig. 3B shows the time course of the radical-scavenging reactions of test compounds at a concentration of 50 μM. The interaction between ABTS and Trolox, the water-soluble α-tocopherol derivative finished within 4 min, and no significant radical-scavenging activities of Trolox were apparent. The reaction of **4** with ABTS was rather slow in comparison to Trolox, and reached a plateau at approximately 4 min after the initiation of the reaction (Fig. 3B). However, compounds **5** and **1** exhibited 68.5 ± 1.6%, and 55.9 ± 1.9% $ABTS^{\cdot+}$ radical-scavenging activities after 4 min of incubation, and 71.4 ± 1.5% and 59 ± 1.7% inhibition of activities after 8 min of incubation. These scavenging activities were found to significantly higher ($p = 0.05$) than that of Trolox (44.1 ± 1.5% ABTS radical-scavenging activity after 8 min of incubation).

4. Conclusions

Antioxidant activities of three different solvent extracts of *Ulva fasciata* Delile were evaluated *in vitro* using DPPH and ABTS assays. The scavenging effect of solvent extracts on the DPPH radical decreased in the order of EtOAc > CH_2Cl_2 > *n*-hexane. The results were found to be similar when tested with ABTS. An 82.6 ± 3.7% radical-scavenging activity was observed for an EtOAc extract at 0.1 mg/ml. EtOAc extract was found to be the most effective free radical scavenger, which was fractionated chromatographically to yield five sesquiterpenoids (**1**–**5**) *viz*., 2,5,5-trimethyl-4-(4′-methyl-3′-pentenyl)-2-cyclohexen-1-ol (**1**), 4-isopentyl-3,4,5,5-tetramethyl-2-cyclohexen-1-ol (**2**), and 4-isopentyl-3,4,5,5-tetramethyl-2-cyclohexen-1-ol (**3**), 6-isopentyl-1,5,5,-tetramethyl-1-cyclohexene (**4**), and 3,4,5,5-tetramethyl-4-(3′-oxopentyl)-2-cyclohexen-1-one (**5**). The structures of the sesquiterpenoids, as well as their relative stereochemistries, were established by means of spectral data analyses, including 2D-NMR experiments. The scavenging effect of the purified compounds decreased with the order: **5** > **1** ≫ **3** > **2** ≫ **4**. Compounds **5** and **1** exhibited effective scavenging activity against DPPH radicals with IC_{50} values of 10.2 and 13.7 mM, respectively. Compound 5 with two carbonyl groups exhibited the highest radical-scavenging capacity (IC_{50} = 10.2 mM). The ABTS scavenging activity of **5** was found to significantly higher (71.4 ± 1.5%) than that of Trolox (44.1 ± 1.5% after 8 min of incubation), and therefore may be a candidate molecule in the food and feed industries.

Acknowledgements

The authors are thankful to Prof. (Dr.) Mohan Joseph Modayil, Director CMFRI, Cochin for providing necessary facilities to carry out the work. Thanks are also due to Dr. Shibu M. Eappen, Scientist B, Sophisticated Test and Instrumentation Centre, Cochin University of Science and Technology, Kerala for recording the mass spectral data.

References

Bandoniene, D., & Murkovic, M. (2002). On-line HPLC–DPPH screening method for evaluation of radical scavenging phenols extracted from apples (*Malus domestica* L.). *Journal of Agricultural and Food Chemistry, 50*, 2482–2487.

Beach, K. S., Smith, C. M., Michael, T. M., & Shin, H. W. (1995). Photosynthesis in reproductive unicells of *Ulva fasciata* and *Enteromorpha flexuosa*: Implications for ecological success. *Marine Ecology Progress Series, 125*, 129–137.

Berge, J. P., Debiton, E., Dumay, J., Durand, P., & Barthomeuf, C. (2002). In vitro anti-inflammatory and anti-proliferative activity of sulfolipids from the red alga *Porphyridium cruentum*. *Journal of Agricultural and Food Chemistry, 50*, 6227–6232.

Bombarda, I., Raharivelomanana, P., Ramanoelina, P. A. R., Faure, R., Bianchini, J. P., & Gaydou, E. M. (2001). Spectrometric identifications of sesquiterpene alcohols from niaouli (*Melaleuca quinquenervia*) essential oil. *Analytica Chimica Acta, 447*, 113–123.

Dykens, J. A., Shick, J. M., Benoit, C., Buettner, G. R., & Winston, G. W. (1992). Oxygen radical production in the sea anemone *Anthopleura elegantissima* and its endosymbiotic algae. *Journal of Experimental Biology, 168*, 219–241.

Faraldos, J. A., Wu, S., Chappell, J., & Coates, R. M. (2007). Conformational analysis of (D)-germacrene A by variabletemperature NMR and NOE spectroscopy. *Tetrahedron, 63*, 7733–7742.

Fayaz, M., Namitha, K. K., Murthy, C. K. N., Swamy, M. M., Sarada, R., Khanam, S., et al. (2005). Chemical composition, iron bioavailability, and antioxidant acativity of *Kappaphycus alvarezzi* (Doty). *Journal of Agricultural and Food Chemistry, 53*, 792–797.

Gray, J. J., Gomaa, E. A., & Buckley, D. J. (1996). Oxidative quality and shelf life of meats. *Meat Science, 43*, 111–123.

Guo, H., Sun, B., Gao, H., Chen, X., Liu, S., Yao, X., et al. (2009). *Diketopiperazines from the Cordyceps colonizing fungus Epicoccum nigrum*. Article ASAP: Journal of Natural products.

Han, K. H., Lee, E. J., & Sung, M. K. (1999). Physical characteristics and antioxidative capacity of major seaweeds. *Journal of Food Science and Nutrition, 4*, 180–183.

Jiménez-Escrig, A., Jiménez-Jiménez, I., Pulido, R., & Saura-Calixto, F. (2001). Antioxidant activity of fresh and processed edible seaweeds. *Journal of Science Food and Agriculture, 81*, 530–534.

Kim, J. M., Araki, S., Kim, D. J., Park, C. P., Takasuka, N., Baba-Toriyama, H., et al. (1998). Chemopreventive effects of carotenoids and curcumins on mouse colon carcinogenesis after 1, 2-dimethylhydrazine initiation. *Carcinogenesis, 19*, 81–85.

Matsukawa, R., Dubinsky, Z., Kishimoto, E., Masaki, K., Masuda, Y., & Takeuchi, T. (1997). A comparison of screening methods for antioxidant activity in seaweeds. *Journal of Applied Phycology, 9*, 29–35.

Mayer, A. M. S., & Lehmann, V. K. B. (2000). Marine pharmacology in 1998: Marine compounds with antibacterial, anticoagulant, anti-inflammatory, anthelmintic, antiplatelet, antiprotozoan, and antiviral activities; with actions on the cardiovascular, endocrine, immune, and nervous systems; and other miscellaneous mechanisms of action. *The Pharmacologist, 42*, 62–69.

Nenadis, N., Wang, L. F., Tsimidou, M., & Zhang, H. Y. (2004). Estimation of scavenging activity of phenolic compounds using the $ABTS^{\cdot}$ assay. *Journal of Agricultural and Food Chemistry, 52*, 4665–4669.

Ozgen, M., Reese, R. N., Tulio, A. Z., Jr, Scheerens, J. C., & Miller, A. R. (2006). Modified 2, 2-azino-bis-3-ethylbenzothiazoline-6-sulfonic Acid method to measure antioxidant capacity of selected small fruits and comparison to ferric reducing antioxidant power and 2, 2'-diphenyl-1-picrylhydrazyl methods. *Journal of Agricultural and Food Chemistry, 54*, 1151–1157.

Ramarathnam, N., Osawa, T., Ochi, H., & Kawakishi, S. (1995). The contribution of plant food antioxidants to human health. *Trends in Food Science and Technology, 6*, 75–82.

Re, R., Pellegrini, N., Proteggente, A., Pannala, A., Yang, M., & Rice-Evans, C. A. (1999). Antioxidant activity applying improved ABTS radical cation decolorization assay. *Free Radical Biology and Medicine, 26*, 1231–1237.

Rezanka, T., Dembitsky, V. M., & Hanus, L. O. (2003). Two cyclohexenone glycosides from the North American fern *Woodwardia virginica* (L.) Smith. *Phytochemistry, 63*, 931–937.

Rouxel, C., Bonnabeze, E., Daniel, A., Jérôme, M., Etienne, M., & Fleurence, J. (2001). Identification by SDS PAGE of green seaweeds (*Ulva* and *Enteromorpha*) used in the food industry. *Journal of Applied Phycology, 13*, 215–218.

Sathivel, A., Raghavendran, H. R. B., Srinivasan, P., & Devaki, T. (2008). Anti-peroxidative and anti-hyperlipidemic nature of *Ulva lactuca* crude polysaccharide on d-galactosamine induced hepatitis in rats. *Food and Chemical Toxicology, 46*, 3262–3267.

Satoru, K., Noboru, T., Hiroo, N., Shinji, S., & Hiroshi, S. (2003). Oversulfation of fucoidan enhances its anti-angiogenic and antitumor activities. *Biochemical Pharmacology, 65*, 173–179.

Shimada, K., Fujikawa, K., Yahara, K., & Nakamura, T. (1992). Antioxidative properties of xanthone on the auto oxidation of soybean in cylcodextrin emulsion. *Journal of Agricultural and Food Chemistry, 40*, 945–948.

Taylor, M. S., & Jacobsen, E. N. (2006). Asymmetric catalysis by chiral hydrogen bond donors. *Angewandte Chemie, 45*, 1520–1543.

Tsang, C., & Kamei, K. Y. (2004). Sargaquinoic acid supports the survival of neuronal PC12D cells in a nerve growth factor-independent manner. *European Journal of Pharmacology, 488*, 11–18.

Wichi, C. M., Kendall, C. W. C., Stamp, D., Medline, A., Archer, M. C., & Bruce, W. R. (1998). Thermally oxidized dietary fat on colon carcinogenesis in rodents. *Nutrtion and Cancer, 30*, 69–73.

Wu, L. C., Ho, J. A., Shieh, M. C., & Lu, I. W. (2005). Antioxidant and antiproliferative activities of spirulina and chlorella water extracts. *Journal of Agricultural and Food Chemistry, 53*, 4207–4212.

Yan, X., Chuda, Y., Suzuki, M., & Nagata, T. (1999). Fucoxanthin as the major antixidant in *Hijikia fusiformis*, a common edible seaweed. *Bioscience Biotechnology and Biochemistry, 63*, 605–607.

Yan, X., Nagata, T., & Fan, X. (1998). Antioxidative activities in some common seaweeds. *Plant Foods for Human Nutrition, 52*, 253–262.